

I am attempting to model solid-state transformations in Inconel 625 based on a published Inconel 718 model [6], which is a generalization of the KKS binary model [3]. Model parameters are listed in Appendix A.

To capture δ , μ , and Laves precipitates in a γ matrix, I have chosen Ni-30% Cr-2% Nb as the model system. The interdendritic regions in additive manufacturing get enriched to Ni-31% Cr-13% Nb. The four-phase three-component model is represented using two composition fields (x_{Cr}, x_{Nb}) and three phase fields ($\phi_\delta, \phi_\mu, \phi_{Laves}$). The CALPHAD database was modified from Du *et al.* [1] to make δ a line compound.

1 Phase Field Model

In this model, the system composition depends on the pure-phase compositions and phase fractions:

$$x_{Cr} = \left(1 - \sum h(|\phi_i|)\right) x_{Cr}^\gamma + h(|\phi_\delta|) x_{Cr}^\delta + h(|\phi_\mu|) x_{Cr}^\mu + h(|\phi_L|) x_{Cr}^L \quad (1)$$

$$x_{Nb} = \left(1 - \sum h(|\phi_i|)\right) x_{Nb}^\gamma + h(|\phi_\delta|) x_{Nb}^\delta + h(|\phi_\mu|) x_{Nb}^\mu + h(|\phi_L|) x_{Nb}^L \quad (2)$$

$$h(\phi) = \phi^3 (6\phi^2 - 15\phi + 10) \quad (3)$$

Therefore, the ternary model is implemented with two “real” compositions (x_{Cr}, x_{Nb}) and eight ‘fictitious’ compositions ($x_{Cr}^\gamma, x_{Nb}^\gamma, x_{Cr}^\delta, x_{Nb}^\delta, x_{Cr}^\mu, x_{Nb}^\mu, x_{Cr}^L, x_{Nb}^L$).

Zhou *et al.* [6] defines the order parameter such that $\phi_i = \pm 1$ indicates presence of the phase i , and $\phi_i = 0$ indicates absence. The matrix phase γ exists where $\sum h(|\phi_i|) = 0$. This allows for multiple discrete precipitates of the same phase, without unphysical coalescence. The free energy density is

$$\begin{aligned} f(x, \phi, t) = & \left(1 - \sum h(|\phi_i|)\right) f_\gamma(x_{Cr}^\gamma, x_{Nb}^\gamma) + h(|\phi_\delta|) f_\delta(x_{Cr}^\delta, x_{Nb}^\delta) + h(|\phi_\mu|) f_\mu(x_{Cr}^\mu, x_{Nb}^\mu) + h(|\phi_L|) f_L(x_{Cr}^L, x_{Nb}^L) \\ & + \omega_\delta (\phi_\delta)^2 (1 - |\phi_\delta|)^2 + \omega_\mu (\phi_\mu)^2 (1 - |\phi_\mu|)^2 + \omega_L (\phi_L)^2 (1 - |\phi_L|)^2 \\ & + \alpha (\phi_\delta^2 \phi_\mu^2 + \phi_\delta^2 \phi_L^2 + \phi_\mu^2 \phi_L^2) \end{aligned} \quad (4)$$

with the elastic energy of the Zhou model neglected here. The first line weighs the single-phase free energy expressions by their respective phase fractions, the second establishes double-well potentials between matrix ($\gamma, \phi = 0$) and the precipitate phases ($\phi = \pm 1$), and the third line penalizes triple junctions and coalescence of precipitate phases.

The KKS interface model [3] assumes constant chemical potential through the interface, so

$$\tilde{\mu}_{Cr} = \frac{\partial f_\gamma}{\partial x_{Cr}^\gamma} = \frac{\partial f_\delta}{\partial x_{Cr}^\delta} = \frac{\partial f_\mu}{\partial x_{Cr}^\mu} = \frac{\partial f_L}{\partial x_{Cr}^L} \quad (5)$$

$$\tilde{\mu}_{Nb} = \frac{\partial f_\gamma}{\partial x_{Nb}^\gamma} = \frac{\partial f_\delta}{\partial x_{Nb}^\delta} = \frac{\partial f_\mu}{\partial x_{Nb}^\mu} = \frac{\partial f_L}{\partial x_{Nb}^L} \quad (6)$$

The pure phase compositions (x_j^i) are determined by solving the parallel tangent construction constrained by the conservation of mass

$$0 = x_{Cr} - \left(1 - \sum h(|\phi_i|)\right) x_{Cr}^\gamma - h(|\phi_\delta|) x_{Cr}^\delta - h(|\phi_\mu|) x_{Cr}^\mu - h(|\phi_L|) x_{Cr}^L \quad (7)$$

$$0 = x_{Nb} - \left(1 - \sum h(|\phi_i|)\right) x_{Nb}^\gamma - h(|\phi_\delta|) x_{Nb}^\delta - h(|\phi_\mu|) x_{Nb}^\mu - h(|\phi_L|) x_{Nb}^L \quad (8)$$

and equality of chemical potentials for each phase,

$$0 = \frac{\partial f_\gamma}{\partial x_{Cr}^\gamma} - \frac{\partial f_\delta}{\partial x_{Cr}^\delta} \quad (9) \quad 0 = \frac{\partial f_\gamma}{\partial x_{Cr}^\gamma} - \frac{\partial f_\mu}{\partial x_{Cr}^\mu} \quad (11) \quad 0 = \frac{\partial f_\gamma}{\partial x_{Cr}^\gamma} - \frac{\partial f_L}{\partial x_{Cr}^L} \quad (13)$$

$$0 = \frac{\partial f_\gamma}{\partial x_{Nb}^\gamma} - \frac{\partial f_\delta}{\partial x_{Nb}^\delta} \quad (10) \quad 0 = \frac{\partial f_\gamma}{\partial x_{Nb}^\gamma} - \frac{\partial f_\mu}{\partial x_{Nb}^\mu} \quad (12) \quad 0 = \frac{\partial f_\gamma}{\partial x_{Nb}^\gamma} - \frac{\partial f_L}{\partial x_{Nb}^L} \quad (14)$$

in which each partial derivative is evaluated at the pure phase composition x_j^i , not the system composition

x_j . This set of eight equations should uniquely solve for the eight unknown pure compositions at each point, given that $x_{\text{Ni}}^i = 1 - x_{\text{Cr}}^i - x_{\text{Nb}}^i$. This solution is found using the GNU Scientific Library's multiroot solver, provided these eight equations and the Jacobian matrix defined by their partial derivatives with respect to $x_{\text{Cr}}^\gamma, x_{\text{Nb}}^\gamma, x_{\text{Cr}}^\delta, x_{\text{Nb}}^\delta, x_{\text{Cr}}^\mu, x_{\text{Nb}}^\mu, x_{\text{Cr}}^L, \text{ and } x_{\text{Nb}}^L$. The complete Jacobian matrix is written in Appendix C.

The first guess for each composition is made using line compound approximations for each phase, applied after the initial condition ($t = 0$). Subsequent guesses simply copy the result of the previous timestep. During the iterations, $x_{\text{Cr}}, x_{\text{Nb}}, \phi_\delta, \phi_\mu, \text{ and } \phi_L$ are held constant. In the event that a valid solution cannot be found, at any time during the simulation, the line compound guesses are applied. Details are provided in Appendix D.

2 Thermodynamic Model

The pure phase free energies depend on Gibbs free energy expressions, divided by molar volume to convert from J/mol to J/m³. The Gibbs free energy expressions are read from a CALPHAD database (Du *et al.* [1]) using pycalphad. This substitution is not valid over the entire ternary composition space, and sometimes incurs kinks.

CALPHAD represents phases in terms of sublattice compositions y , not system compositions x . This is fundamental to CALPHAD. Each sublattice has a site fraction a , similar to the subscripts in a molecular formula. The sublattice compositions are constrained by mass conservation:

$$a' + a'' + \dots = 1 \quad (15)$$

$$\begin{aligned} a'y'_A + a''y''_A + \dots &= x_A \\ a'y'_B + a''y''_B + \dots &= x_B \end{aligned} \quad (16)$$

where ' indicates the first sublattice, '' the second, etc. The lattice fractions are also conserved:

$$\begin{aligned} y'_A + y'_B + \dots &= 1 \\ y''_A + y''_B + \dots &= 1 \end{aligned} \quad (17)$$

These constraints can, for some phases, be used to map sublattice compositions directly into system compositions. If all but one component appear on only one sublattice each, then y maps into x uniquely.

- γ is represented with one sublattice [1], (Cr,Nb,Ni)₁. This maps trivially:

$$\begin{aligned} y'_{\text{Cr}} &= x_{\text{Cr}} \\ y'_{\text{Nb}} &= x_{\text{Nb}} \\ y'_{\text{Ni}} &= x_{\text{Ni}} \end{aligned}$$

- δ is represented with two sublattices [1], (Nb,Ni)_{1/4}(Cr,Nb,Ni)_{3/4}. Since Nb and Ni appear on both, this cannot be mapped. However, if we assume that Nb partitions to the first sublattice, (Nb,Ni)_{1/4}(Cr,Ni)_{3/4} can be solved.

$$\begin{aligned} y'_{\text{Nb}} &= 4x_{\text{Nb}} & y''_{\text{Cr}} &= \frac{4}{3}x_{\text{Cr}} & x_{\text{Cr}} &< \frac{3}{4} \\ y'_{\text{Ni}} &= 1 - 4x_{\text{Nb}} & y''_{\text{Ni}} &= 1 - \frac{4}{3}x_{\text{Cr}} & x_{\text{Nb}} &< \frac{1}{4} \end{aligned}$$

- μ is represented with two sublattices $[1]$, $\text{Nb}_{6/13}(\text{Cr}, \text{Nb}, \text{Ni})_{7/13}$. This maps readily:

$$\begin{aligned}
 y''_{\text{Cr}} &= \frac{13}{7} x_{\text{Cr}} & x_{\text{Cr}} &< \frac{7}{13} \\
 y'_{\text{Nb}} &= 1 & y''_{\text{Nb}} &= \frac{13}{7} x_{\text{Nb}} - \frac{6}{7} & x_{\text{Nb}} &> \frac{6}{13} \\
 y''_{\text{Ni}} &= \frac{13}{7} x_{\text{Ni}} & x_{\text{Ni}} &< \frac{7}{13}
 \end{aligned}$$

- Laves is represented with two sublattices, $(\text{Cr}, \text{Nb}, \text{Ni})_{2/3}(\text{Cr}, \text{Nb})_{1/3}$. Since Cr and Nb appear on both sublattices, this cannot be mapped. Again, assuming that Nb partitions to the second lattice, $(\text{Cr}, \text{Ni})_{2/3}(\text{Cr}, \text{Nb})_{1/3}$ can be solved.

$$\begin{aligned}
 y'_{\text{Cr}} &= 1 - \frac{3}{2} x_{\text{Ni}} & y''_{\text{Cr}} &= 1 - 3x_{\text{Nb}} \\
 y'_{\text{Ni}} &= \frac{3}{2} x_{\text{Ni}} & y''_{\text{Nb}} &= 3x_{\text{Nb}} & x_{\text{Nb}} &< \frac{1}{3} \\
 & & & & x_{\text{Ni}} &< \frac{2}{3}
 \end{aligned}$$

2.1 Taylor series approximation

Since smooth and continuously differentiable functions are needed, the single-phase free energies are approximated by second-order Taylor series expansion about control compositions $\mathbf{a} = (a_{\text{Cr}}, a_{\text{Nb}}, a_{\text{Ni}})$ chosen empirically such that the phase diagram is qualitatively correct (Fig. 1). For each phase $\alpha \in (\gamma, \delta, \mu, \text{Laves})$,

$$\begin{aligned}
 f_{\alpha} &\approx f_{\alpha}(a_{\text{Cr}}^{\alpha}, a_{\text{Nb}}^{\alpha}) \\
 &+ \sum_i \frac{\partial f_{\alpha}(a_{\text{Cr}}^{\alpha}, a_{\text{Nb}}^{\alpha})}{\partial x_i^{\alpha}} (x_i^{\alpha} - a_i^{\alpha}) \\
 &+ \sum_i \sum_j \frac{1}{2} \frac{\partial^2 f_{\alpha}(a_{\text{Cr}}^{\alpha}, a_{\text{Nb}}^{\alpha})}{\partial x_i^{\alpha} \partial x_j^{\alpha}} (x_i^{\alpha} - a_i^{\alpha}) (x_j^{\alpha} - a_j^{\alpha})
 \end{aligned} \tag{18}$$

with $i, j \in \text{Cr}, \text{Nb}, \text{Ni}$. Note that, depending on the CALPHAD expression, some terms are null for each phase.

2.2 Continuous and Differentiable Boundaries

The KKS interface model [3] requires the free energy landscape for each phase to be smooth, continuous, and differentiable everywhere. In the CALPHAD database, however, the sublattice description introduces bounds on the valid domain for each phase, outside of which the free energy is undefined. We therefore construct a “funnel” around each CALPHAD free energy to help numerical methods gone astray to find their way back inside the valid domain. For simplicity, the funnels are constructed using independent linear functions of one composition each, stitched together using hyperbolic tangent (tanh) functions. These interpolate through an exclusion zone of width α around the border of each valid domain, guaranteeing continuity and differentiability.

For an arbitrary CALPHAD model with a constraint on only one composition, the free energy landscape is stitched together from the CALPHAD expression $G(x)$ and the funnel expression $V(x)$ with critical composition x^* . Considering Fig. 2, a tanh function is applied to interpolate between G (parabolic, on the

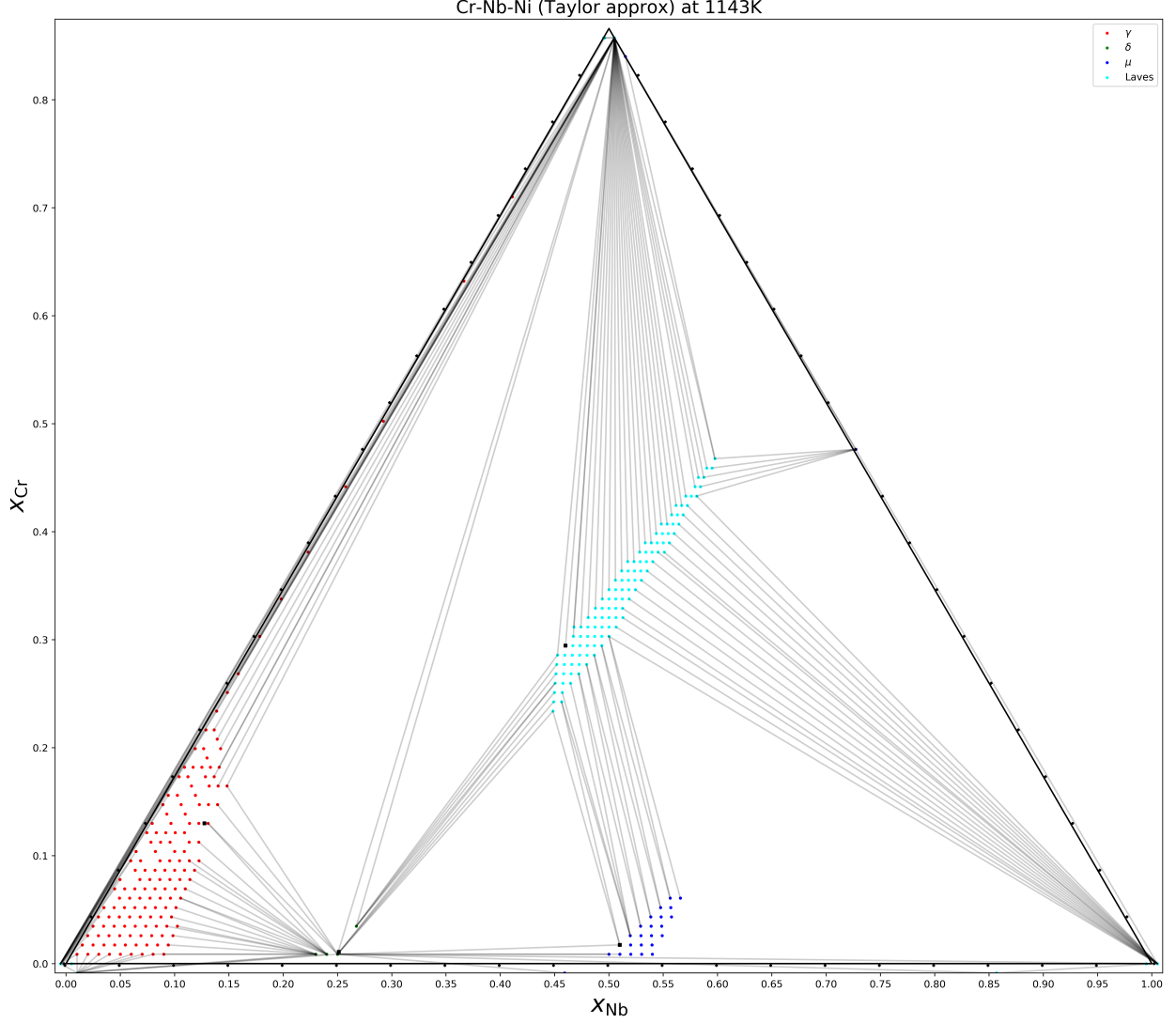


Figure 1: Phase diagram produced by a convex hull algorithm. Lines in coexistence regions are schematic, being edges of hull facets rather than thermodynamic tie lines. Black points inside the ternary simplex indicate control points $(a_{\text{Cr}}, a_{\text{Nb}}, a_{\text{Ni}})$ for the Taylor series expansions. The $\gamma - \delta - \text{Laves}$ and $\delta - \mu - \text{Laves}$ three-phase coexistence regions are qualitatively correct, but the phase boundaries are displaced and distorted relative to Du *et al.* [1].

left) and V (linear, on the right) as follows:

$$\begin{aligned} \xi &= \frac{2\pi}{\alpha} \left(x - x^* - \frac{\alpha}{2} \right) \\ V(x) &= \max(G(x)) + \frac{1}{4} (\max(G(x)) - \min(G(x))) (x - x^*) \end{aligned} \quad (19)$$

$$\begin{aligned} F(x) &= G(x) + \frac{1}{2} (V(x) - G(x)) [1 + \tanh \xi] \\ &= \frac{1}{2} [1 - \tanh \xi] G(x) + \frac{1}{2} [1 + \tanh \xi] V(x). \end{aligned} \quad (20)$$

With constraints on two compositions,

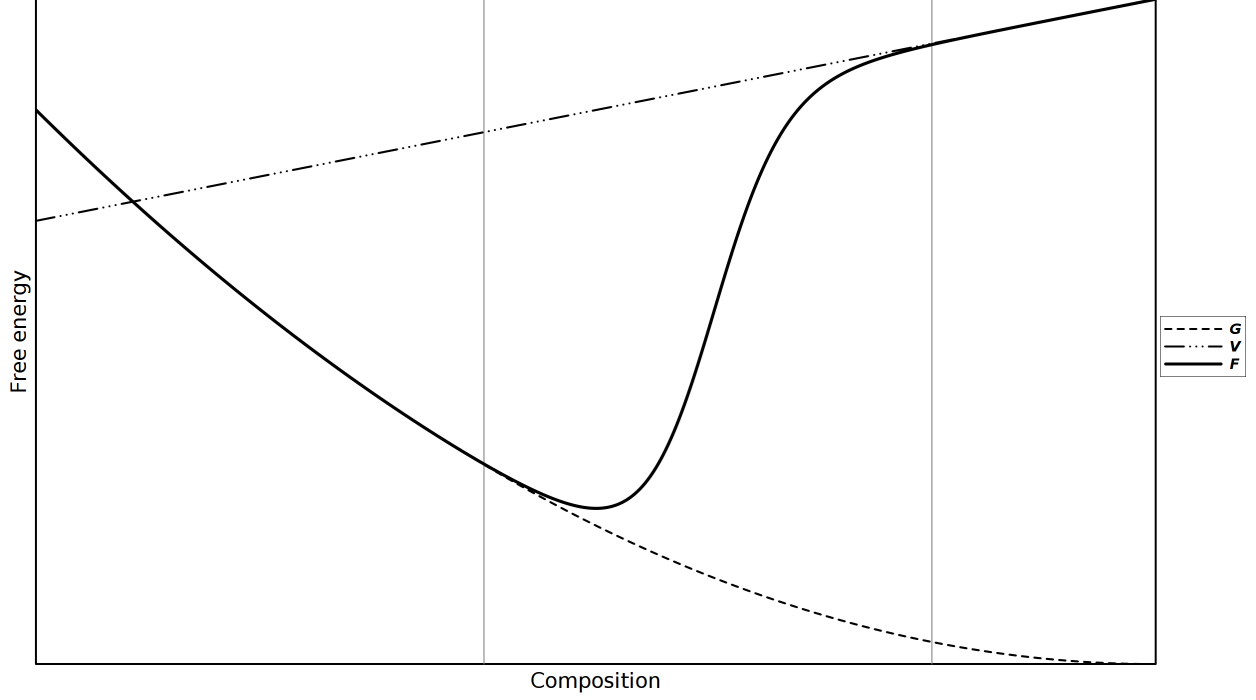


Figure 2: Schematic interpolation between the CALPHAD free energy $G(x)$ and a funnel potential $V(x)$ using a hyperbolic tangent function over a finite composition $\Delta x = \alpha$, shown between the vertical lines. The splined function $F(x)$ is smooth, continuous, and differentiable everywhere.

$$\xi_i = \frac{2\pi}{\alpha} \left(x_i - x_i^* - \frac{\alpha}{2} \right) \quad (21)$$

$$\begin{aligned} F(x_1, x_2) &= G(x_1, x_2) + \frac{1}{2} (V(x_1) - G(x_1, x_2)) [1 + \tanh \xi_1] + \frac{1}{2} (V(x_2) - G(x_1, x_2)) [1 + \tanh \xi_2] \\ &= \frac{1}{2} [-\tanh \xi_1 - \tanh \xi_2] G(x_1, x_2) + \frac{1}{2} [1 + \tanh \xi_1] V(x_1) + \frac{1}{2} [1 + \tanh \xi_2] V(x_2). \end{aligned} \quad (22)$$

Generalizing to constraints on N compositions, and adding terms to cancel undesirable contributions in regions where more than one funnel function is active,¹

$$\begin{aligned} F(\vec{x}) &= \frac{1}{2} \left[2 - N - \sum_{i=1}^N \tanh \xi_i + \frac{1}{2} \sum_{i=1}^N \sum_{j>i}^N (1 + \tanh \xi_i) (1 + \tanh \xi_j) \right] G(\vec{x}) \\ &\quad + \frac{1}{2} \sum_{i=1}^N \left[(1 + \tanh \xi_i) - \frac{1}{4} \sum_{j>i}^N (1 + \tanh \xi_i) (1 + \tanh \xi_j) \right] V(x_i). \end{aligned} \quad (23)$$

For a “high-side” constraint, e.g. approaching $x_{\text{Cr}}^* = 1$ from inside the simplex, α should be positive in the definition of ξ (Eqn. 21). For a “low-side” constraint, e.g. approaching $x_{\text{Cr}}^* = 0$ from inside the simplex, α should be negative. No other changes are necessary to reverse directionality of the tanh profiles.

¹The double-summation in the coefficient of $G(\vec{x})$ removes an extraneous term of $-G(\vec{x})$ in “corners”, while the sum over j in the coefficient of $V(x_i)$ produces the average $\frac{1}{2}[V(x_i) + V(x_j)]$ instead of the full sum of $V(x_i) + V(x_j)$ in those regions.

3 Equations of Motion for Phases $\{\phi\}$

The $\{\phi_i\}$ are not conserved, so Allen-Cahn dynamics are assumed:

$$\frac{\partial \phi_i}{\partial t} = -L_i \frac{\delta \mathcal{F}}{\delta \phi_i} = -L_i \left(\frac{\partial f}{\partial \phi_i} - \kappa_i \nabla^2 \phi_i \right). \quad (24)$$

From Eqn. 4,

$$\begin{aligned} \frac{\partial f}{\partial \phi_n} = & -\text{sgn}(\phi_i) h'(|\phi_n|) [f_\gamma(x_{\text{Cr}}^\gamma, x_{\text{Nb}}^\gamma) - f_n(x_{\text{Cr}}^n, x_{\text{Nb}}^n)] + \left[1 - \sum h(|\phi_i|) \right] \frac{\partial f_\gamma}{\partial \phi_n} + h(|\phi_n|) \frac{\partial f_n}{\partial \phi_n} \\ & + 2\omega_n \phi_n (1 - |\phi_n|)^2 - 2\omega_n \phi_n^2 \text{sgn}(\phi_n) (1 - |\phi_n|) + 2\alpha \phi_n \sum_{i \neq n} \phi_i^2. \end{aligned} \quad (25)$$

Invoking the multivariable chain rule and chemical potential (Eqns. 5 and 6),

$$\begin{aligned} \frac{\partial f_\alpha}{\partial \phi_\alpha} = & \sum_j \frac{\partial f_\alpha}{\partial x_j^\alpha} \frac{\partial x_j^\alpha}{\partial \phi_\alpha} = \sum_j \frac{\partial x_j^\alpha}{\partial \phi_\alpha} \tilde{\mu}_j \\ \frac{\partial f}{\partial \phi_n} = & -\text{sgn}(\phi_n) h'(|\phi_n|) [f_\gamma(x_{\text{Cr}}^\gamma, x_{\text{Nb}}^\gamma) - f_n(x_{\text{Cr}}^n, x_{\text{Nb}}^n)] + \sum_j \left(\left[1 - \sum h(|\phi_i|) \right] \frac{\partial x_j^\gamma}{\partial \phi_n} + h(|\phi_n|) \frac{\partial x_j^n}{\partial \phi_n} \right) \tilde{\mu}_j \\ & + 2\omega_n \phi_n (1 - |\phi_n|) [1 - h(|\phi_n|) - \text{sgn}(\phi_n) \phi_n] + 2\alpha \phi_n \sum_{i \neq n} \phi_i^2. \end{aligned} \quad (26)$$

Implicitly differentiating both sides of the expression for system composition, Eqns. 1 and 2, with respect to a phase,²

$$\frac{\partial x_j}{\partial \phi_n} = -\text{sgn}(\phi_n) h'(|\phi_n|) [x_j^\gamma - x_j^n] + \left[1 - \sum h(|\phi_i|) \right] \frac{\partial x_j^\gamma}{\partial \phi_n} + h(|\phi_n|) \frac{\partial x_j^n}{\partial \phi_n} \quad (27)$$

$$\frac{\partial x_j}{\partial \phi_n} \equiv 0 \quad (28)$$

$$\text{sgn}(\phi_n) h'(|\phi_n|) [x_j^\gamma - x_j^n] = \left[1 - \sum h(|\phi_i|) \right] \frac{\partial x_j^\gamma}{\partial \phi_n} + h(|\phi_n|) \frac{\partial x_j^n}{\partial \phi_n}. \quad (29)$$

Substituting Eqn. 29 into Eqn. 26 and simplifying, we arrive at the final result:

$$\begin{aligned} \frac{\partial f}{\partial \phi_n} = & -\text{sgn}(\phi_n) h'(|\phi_n|) \left(f_\gamma(x_{\text{Cr}}^\gamma, x_{\text{Nb}}^\gamma) - f_n(x_{\text{Cr}}^n, x_{\text{Nb}}^n) - \sum_j [x_j^\gamma - x_j^n] \tilde{\mu}_j \right) \\ & + 2\omega_n \phi_n (1 - |\phi_n|) [1 - h(|\phi_n|) - \text{sgn}(\phi_n) \phi_n] + 2\alpha \phi_n \sum_{i \neq n} \phi_i^2. \end{aligned} \quad (30)$$

4 Equations of Motion for Compositions $\{x\}$

Composition is conserved, so we choose Cahn-Hilliard dynamics for x :

$$\frac{\partial x_\ell}{\partial t} = \nabla \cdot \sum_k M_{\ell k} \nabla \frac{\delta \mathcal{F}}{\delta x_k} = \nabla \cdot \sum_k M_{\ell k} \nabla \frac{\partial f}{\partial x_k}. \quad (31)$$

²Cf. Eqn. 6.91 in Provatas and Elder [4]. The amount of species should not change explicitly with changes in phase.

Differentiating Eqn. 4, then applying the chain rule and the definition of chemical potential,

$$\frac{\partial f}{\partial x_k} = \left[1 - \sum_{\alpha} h(|\phi_{\alpha}|) \right] \frac{\partial f_{\gamma}}{\partial x_k} + \sum_{\alpha} h(|\phi_{\alpha}|) \frac{\partial f_{\alpha}}{\partial x_k} \quad (32)$$

$$= \sum_j \left[1 - \sum_{\alpha} h(|\phi_{\alpha}|) \right] \frac{\partial f_{\gamma}}{\partial x_j^{\gamma}} \frac{\partial x_j^{\gamma}}{\partial x_k} + \sum_j \sum_{\alpha} h(|\phi_{\alpha}|) \frac{\partial f_{\alpha}}{\partial x_j^{\alpha}} \frac{\partial x_j^{\alpha}}{\partial x_k} \quad (33)$$

$$= \sum_j \left(\left[1 - \sum_{\alpha} h(|\phi_{\alpha}|) \right] \frac{\partial x_j^{\gamma}}{\partial x_k} \mu_j^{\gamma} + \sum_{\alpha} h(|\phi_{\alpha}|) \frac{\partial x_j^{\alpha}}{\partial x_k} \mu_j^{\alpha} \right). \quad (34)$$

Since the pure-phase composition x_j^{α} depends only on x_j , $\frac{\partial x_j^{\alpha}}{\partial x_k} = \delta_{jk}$, and

$$\frac{\partial f}{\partial x_k} = \left[1 - \sum_{\alpha} h(|\phi_{\alpha}|) \right] \mu_k^{\gamma} + \sum_{\alpha} h(|\phi_{\alpha}|) \mu_k^{\alpha}. \quad (35)$$

In this phase field formulation, $\tilde{\mu}_k \equiv \mu_k^{\gamma} = \mu_k^{\alpha}$ (Eqn. 5) and

$$\frac{\partial f}{\partial x_k} = \tilde{\mu}_k. \quad (36)$$

Substituting Eqn. 36 into Eqn. 31, with a proportionality constant V_m^2 , we

$$\frac{\partial x_{\ell}}{\partial t} = V_m^2 \nabla \cdot \sum_k M_{\ell k} \nabla \tilde{\mu}_k. \quad (37)$$

Since we do not have detailed interfacial data, the mobility matrix is diagonal and $M_{\ell k} = \delta_{\ell k} M_{\ell}$, *i.e.* the mobility of element ℓ only depends on its own concentration field. Using this simplification, we can recover the form presented by Zhou *et al.* [6]:

$$\frac{\partial x_{\ell}}{\partial t} = V_m^2 \nabla \cdot M_{\ell} \nabla \tilde{\mu}_k. \quad (38)$$

If we further invoke the chain rule,

$$\frac{\partial x_{\ell}}{\partial t} = V_m^2 \nabla \cdot M_{\ell} \sum_j \frac{\partial \tilde{\mu}_k}{\partial x_j^{\gamma}} \nabla x_j^{\gamma} \quad (39)$$

$$= V_m^2 \nabla \cdot M_{\ell} \sum_j \frac{\partial^2 f_{\gamma}}{\partial x_{\ell}^{\gamma} \partial x_j^{\gamma}} \nabla x_j^{\gamma} \quad (40)$$

For the specific case of paraboloid approximations to the pure free energy expressions, the cross-terms of curvature are zero, and we have an equivalent result in terms of composition rather than chemical potential:

$$\frac{\partial x_{\ell}}{\partial t} = 2V_m^2 \nabla \cdot M_{\ell} C_{\ell}^{\gamma} \nabla x_{\ell}^{\gamma}, \quad (41)$$

with curvature $C_{\ell}^{\gamma} = \frac{1}{2} \frac{\partial^2 f_{\gamma}}{\partial (x_{\ell}^{\gamma})^2}$.

We can also use the definition of diffusivity:

$$D_{\ell j}^{\alpha} = \sum_k M_{\ell k}^{\alpha} \frac{\partial^2 f_{\gamma}}{\partial x_{\ell}^{\alpha} \partial x_j^{\alpha}} \quad (42)$$

$$\frac{\partial x_{\ell}}{\partial t} = \nabla \cdot \sum_j D_{\ell j}^{\gamma} \nabla x_j^{\gamma}. \quad (43)$$

For Cr–Nb–Ni, we have diffusivity data at 1273 K [5]; for a matrix of Ni–26.4 % Cr–1.3 % Nb,

$$\tilde{D}^{\text{Ni}} = \begin{bmatrix} \tilde{D}_{\text{CrCr}} & \tilde{D}_{\text{CrNb}} \\ \tilde{D}_{\text{NbCr}} & \tilde{D}_{\text{NbNb}} \end{bmatrix} = \begin{bmatrix} 2.16 & 2.97 \\ 0.56 & 4.29 \end{bmatrix} \times 10^{-15} \text{ m}^2 \text{ s}^{-1}. \quad (44)$$

If we treat diffusivity as temperature-independent, then

$$\frac{\partial x_\ell}{\partial t} = D_{\ell\text{Cr}}^\gamma \nabla^2 x_{\text{Cr}}^\gamma + D_{\ell\text{Nb}}^\gamma \nabla^2 x_{\text{Nb}}^\gamma. \quad (45)$$

5 Timestep Adaptivity

If the phase-field ϕ advances more than one mesh point in a given timestep, the solution is unstable. In practice, ϕ should advance $0.1\Delta x$ or less. Using the advection equation,

$$\frac{\Delta\phi}{\Delta t} = u|\nabla\phi| \quad (46)$$

with velocity u normal to the interface, we can take a step $\Delta t < \frac{(\Delta x)^2}{4D}$ and solve for

$$\Delta t^* = \frac{0.1\Delta x}{u}, \quad (47)$$

the timestep we “should” have taken to move the interface as quickly as possible. If the global maximum Δt^* is smaller than the actual Δt , we can speed up for the next step. Otherwise, if $\Delta t > \Delta t^*$, the current step is invalid and must be repeated with a smaller timestep. Useful scaling factors were empirically found to be $1.00001\Delta t$ to accelerate and $0.9\Delta t$ to brake, although braking is best avoided.

A Model parameters

Table 1: Model parameters used in this work

Parameter	Symbol	Value
Mesh resolution	Δx	5.0×10^{-9} m
Timestep	Δt	5.0×10^{-7} s
Temperature	T	870 °C
Molar volume	V_m	1.0×10^{-5} m ³ /mol
Trijunction penalty	α	1.07×10^{11} J/m ³
Interfacial energy	$\sigma_\delta = \sigma_\mu = \sigma_L$	1.01 J/m ²
Gradient penalty	$\kappa_\delta = \kappa_\mu = \kappa_L$	1.24×10^{-8} J/m
Mobility	$M_{Cr} = M_{Nb}$	2.42×10^{-18} mol ² /Nsm ²
Diffusivity	$D_{Cr} = D_{Nb}$	1.58×10^{-16} m ² /s
Mobility	$L_\delta = L_\mu = L_L$	2.904×10^{-11} m ² /N/s
Interface width	2λ	$7\Delta x$
Interface width	2λ	35×10^{-9} m
Well height	$\omega_\delta = \omega_\mu = \omega_L$	$6.6\sigma_\delta/2\lambda$
Well height	$\omega_\delta = \omega_\mu = \omega_L$	1.9×10^8 J/m ³
γ curvature	C_{Cr}^γ	4.8×10^{10} J/m ³
	C_{Nb}^γ	6.1×10^9 J/m ³
δ curvature	C_{Cr}^δ	5.4×10^{10} J/m ³
	C_{Nb}^δ	6.8×10^{11} J/m ³
μ curvature	C_{Cr}^μ	4.5×10^{10} J/m ³
	C_{Nb}^μ	2.1×10^{10} J/m ³
Laves curvature	C_{Nb}^L	1.2×10^{11} J/m ³
	C_{Ni}^L	1.1×10^{10} J/m ³
γ composition	$^e x_{Cr}^\gamma$	1.00 %
	$^e x_{Nb}^\gamma$	32.3 %
δ composition	$^e x_{Cr}^\delta$	0.88 %
	$^e x_{Nb}^\delta$	24.9 %
μ composition	$^e x_{Cr}^\mu$	1.06 %
	$^e x_{Nb}^\mu$	50.8 %
Laves composition	$^e x_{Nb}^L$	30.6 %
	$^e x_{Ni}^L$	49.1 %
γ minimum	$f_\gamma^0(^e x_{Cr}^\gamma, ^e x_{Nb}^\gamma)$	-7.9722×10^9 J/m ³
δ minimum	$f_\delta^0(^e x_{Cr}^\delta, ^e x_{Nb}^\delta)$	-8.5488×10^9 J/m ³
μ minimum	$f_\mu^0(^e x_{Cr}^\mu, ^e x_{Nb}^\mu)$	-8.0076×10^9 J/m ³
Laves minimum	$f_L^0(^e x_{Nb}^L, ^e x_{Ni}^L)$	-8.0522×10^9 J/m ³

B Units of the Diffusion Equations

The expression $\frac{\partial x}{\partial t}$ should have units of s⁻¹. For Eqn. 44, this is clearly so:

$$\begin{aligned} \frac{1}{s} &= \frac{m^2}{s} \frac{1}{m^2} \\ &= \frac{1}{s}. \end{aligned}$$

The unusual units in Eqn. 38 make the equivalence just slightly less obvious, but it is straightforward

nonetheless:

$$\begin{aligned} \frac{1}{s} &= \frac{\text{m}^6}{\text{mol}^2} \frac{\text{mol}^2}{\text{N s m}^2} \frac{\text{J}}{\text{m}^3 \text{m}^2} = \frac{\text{m}^6}{\text{mol}^2} \frac{\text{mol}^2 \text{s}^2}{\text{kg m s m}^2} \frac{\text{kg m}^2}{\text{m}^3 \text{m}^2 \text{s}^2} = \frac{\text{kg m}^8 \text{s}^2 \text{mol}^2}{\text{kg m}^8 \text{s}^3 \text{mol}^2} \\ &= \frac{1}{s}. \end{aligned}$$

Eqns. 38, 41, and 44 are interchangeable, simply adjust the timestep to satisfy

$$\Delta t < \min \left(\frac{(\Delta x)^2}{8V_m^2 M_{\text{Nb}} C_{\text{Nb}}^\gamma}, \frac{(\Delta x)^2}{4D_{\text{Nb}}} \right).$$

C Common Tangent

The Jacobian matrix $\left(J_{ij} = \frac{\partial f_i}{\partial x_j} \right)$ for this system of eight equations, depending on the eight unknown compositions $\{x_{\text{Cr}}^i\}, \{x_{\text{Nb}}^i\}$, is written

J_{ij}	$\partial x_{\text{Cr}}^\gamma$	$\partial x_{\text{Nb}}^\gamma$	$\partial x_{\text{Cr}}^\delta$	$\partial x_{\text{Nb}}^\delta$	$\partial x_{\text{Cr}}^\mu$	$\partial x_{\text{Nb}}^\mu$	$\partial x_{\text{Cr}}^{\text{L}}$	$\partial x_{\text{Nb}}^{\text{L}}$
$\partial(\text{Eqn. 7})$	$-1 + \sum h(\phi_i)$	0	$-h(\phi_\delta)$	0	$-h(\phi_\mu)$	0	$-h(\phi_{\text{L}})$	0
$\partial(\text{Eqn. 8})$	0	$-1 + \sum h(\phi_i)$	0	$-h(\phi_\delta)$	0	$-h(\phi_\mu)$	0	$-h(\phi_{\text{L}})$
$\partial(\text{Eqn. 9})$	$\frac{\partial^2 f_\gamma}{\partial (x_{\text{Cr}}^\gamma)^2}$	$\frac{\partial^2 f_\gamma}{\partial x_{\text{Cr}}^\gamma \partial x_{\text{Nb}}^\gamma}$	$\frac{\partial^2 f_\delta}{\partial (x_{\text{Cr}}^\delta)^2}$	$\frac{\partial^2 f_\delta}{\partial x_{\text{Cr}}^\delta \partial x_{\text{Nb}}^\delta}$	0	0	0	0
$\partial(\text{Eqn. 10})$	$\frac{\partial^2 f_\gamma}{\partial x_{\text{Nb}}^\gamma \partial x_{\text{Cr}}^\gamma}$	$\frac{\partial^2 f_\gamma}{\partial (x_{\text{Nb}}^\gamma)^2}$	$\frac{\partial^2 f_\delta}{\partial x_{\text{Nb}}^\delta \partial x_{\text{Cr}}^\delta}$	$\frac{\partial^2 f_\delta}{\partial (x_{\text{Nb}}^\delta)^2}$	0	0	0	0
$\partial(\text{Eqn. 11})$	$\frac{\partial^2 f_\gamma}{\partial (x_{\text{Cr}}^\gamma)^2}$	$\frac{\partial^2 f_\gamma}{\partial x_{\text{Cr}}^\gamma \partial x_{\text{Nb}}^\gamma}$	0	0	$\frac{\partial^2 f_\mu}{\partial (x_{\text{Cr}}^\mu)^2}$	$\frac{\partial^2 f_\mu}{\partial x_{\text{Cr}}^\mu \partial x_{\text{Nb}}^\mu}$	0	0
$\partial(\text{Eqn. 12})$	$\frac{\partial^2 f_\gamma}{\partial x_{\text{Nb}}^\gamma \partial x_{\text{Cr}}^\gamma}$	$\frac{\partial^2 f_\gamma}{\partial (x_{\text{Nb}}^\gamma)^2}$	0	0	$\frac{\partial^2 f_\mu}{\partial x_{\text{Nb}}^\mu \partial x_{\text{Cr}}^\mu}$	$\frac{\partial^2 f_\mu}{\partial (x_{\text{Nb}}^\mu)^2}$	0	0
$\partial(\text{Eqn. 13})$	$\frac{\partial^2 f_\gamma}{\partial (x_{\text{Cr}}^\gamma)^2}$	$\frac{\partial^2 f_\gamma}{\partial x_{\text{Cr}}^\gamma \partial x_{\text{Nb}}^\gamma}$	0	0	0	0	$\frac{\partial^2 f_{\text{L}}}{\partial (x_{\text{Cr}}^{\text{L}})^2}$	$\frac{\partial^2 f_{\text{L}}}{\partial x_{\text{Cr}}^{\text{L}} \partial x_{\text{Nb}}^{\text{L}}}$
$\partial(\text{Eqn. 14})$	$\frac{\partial^2 f_\gamma}{\partial x_{\text{Nb}}^\gamma \partial x_{\text{Cr}}^\gamma}$	$\frac{\partial^2 f_\gamma}{\partial (x_{\text{Nb}}^\gamma)^2}$	0	0	0	0	$\frac{\partial^2 f_{\text{L}}}{\partial x_{\text{Nb}}^{\text{L}} \partial x_{\text{Cr}}^{\text{L}}}$	$\frac{\partial^2 f_{\text{L}}}{\partial (x_{\text{Nb}}^{\text{L}})^2}$

For the specific case of paraboloid approximations for the pure phase free energies, the matrix reduces to

J_{ij}	$\partial x_{\text{Cr}}^\gamma$	$\partial x_{\text{Nb}}^\gamma$	$\partial x_{\text{Cr}}^\delta$	$\partial x_{\text{Nb}}^\delta$	$\partial x_{\text{Cr}}^\mu$	$\partial x_{\text{Nb}}^\mu$	$\partial x_{\text{Cr}}^{\text{L}}$	$\partial x_{\text{Nb}}^{\text{L}}$
$\partial(\text{Eqn. 7})$	$-1 + \sum h(\phi_i)$	0	$-h(\phi_\delta)$	0	$-h(\phi_\mu)$	0	$-h(\phi_{\text{L}})$	0
$\partial(\text{Eqn. 8})$	0	$-1 + \sum h(\phi_i)$	0	$-h(\phi_\delta)$	0	$-h(\phi_\mu)$	0	$-h(\phi_{\text{L}})$
$\partial(\text{Eqn. 9})$	$2C_{\text{Cr}}^\gamma$	0	$2C_{\text{Cr}}^\delta$	0	0	0	0	0
$\partial(\text{Eqn. 10})$	0	$2C_{\text{Nb}}^\gamma$	0	$2C_{\text{Nb}}^\delta$	0	0	0	0
$\partial(\text{Eqn. 11})$	$2C_{\text{Cr}}^\gamma$	0	0	0	$2C_{\text{Cr}}^\mu$	0	0	0
$\partial(\text{Eqn. 12})$	0	$2C_{\text{Nb}}^\gamma$	0	0	0	$2C_{\text{Nb}}^\mu$	0	0
$\partial(\text{Eqn. 13})$	$2C_{\text{Cr}}^\gamma$	0	0	0	0	0	$\frac{\partial^2 f_{\text{L}}}{\partial (x_{\text{Cr}}^{\text{L}})^2}$	$\frac{\partial^2 f_{\text{L}}}{\partial x_{\text{Cr}}^{\text{L}} \partial x_{\text{Nb}}^{\text{L}}}$
$\partial(\text{Eqn. 14})$	0	$2C_{\text{Nb}}^\gamma$	0	0	0	0	$\frac{\partial^2 f_{\text{L}}}{\partial x_{\text{Nb}}^{\text{L}} \partial x_{\text{Cr}}^{\text{L}}}$	$\frac{\partial^2 f_{\text{L}}}{\partial (x_{\text{Nb}}^{\text{L}})^2}$

D Line Compound Approximations

Initial guesses, and replacement values for parallel tangent iterations which fail to converge, are made using line compound approximations based on the pure phase regions observed on the Cr–Nb–Ni phase diagram. Specifically, the composition of one species is set equal to a constant value, and the other two are scaled from their “real” values (as opposed to the “fictitious” quantities being solved for) to satisfy conservation of mass in each point ($\sum x_i = 1$). Replacements for un-converged values are perturbed with random noise of amplitude $\varepsilon = 10^{-5}$.

$$\begin{aligned}
x_{\text{Nb}}^{\gamma} &= 0.015 \\
x_{\text{Cr}}^{\gamma} &= \frac{x_{\text{Cr}}}{x_{\text{Cr}} + x_{\text{Nb}}^{\gamma} + x_{\text{Ni}}} \\
&= \frac{x_{\text{Cr}}}{1 + x_{\text{Nb}}^{\gamma} - x_{\text{Nb}}}
\end{aligned}$$

$$\begin{aligned}
x_{\text{Ni}}^{\delta} &= 0.75 \\
x_{\text{Cr}}^{\delta} &= \frac{x_{\text{Cr}}}{x_{\text{Cr}} + x_{\text{Nb}} + x_{\text{Ni}}^{\delta}} \\
x_{\text{Nb}}^{\delta} &= \frac{x_{\text{Nb}}}{x_{\text{Cr}} + x_{\text{Nb}} + x_{\text{Ni}}^{\delta}}
\end{aligned}$$

$$\begin{aligned}
x_{\text{Nb}}^{\mu} &= 0.525 \\
x_{\text{Cr}}^{\mu} &= \frac{x_{\text{Cr}}}{1 + x_{\text{Nb}}^{\mu} - x_{\text{Nb}}}
\end{aligned}$$

$$\begin{aligned}
x_{\text{Nb}}^{\text{L}} &= 0.30 \\
x_{\text{Cr}}^{\text{L}} &= \frac{x_{\text{Cr}}}{1 + x_{\text{Nb}}^{\text{L}} - x_{\text{Nb}}}
\end{aligned}$$

References

- [1] Du, Y.; Liu, S.; Chang, Y. A.; and Yang, Y. “A Thermodynamic Modeling of the Cr–Nb–Ni System.” *Calphad* **29** (2005) 140–148. DOI: 10.1016/j.calphad.2005.06.001.
- [2] Karunaratne, M. S. A. and Reed, R. C. “Interdiffusion of Niobium and Molybdenum in Nickel between 900 - 1300 °C.” *Defect and Diffusion Forum* **237-240** (2005) 420–425. DOI: 10.4028/www.scientific.net/DDF.237-240.420.
- [3] Kim, S. G.; Kim, W. T. and Suzuki, T. “Phase-field model for binary alloys.” *Phys. Rev. E* **60** (1999) 7186–7197. DOI: 10.1103/PhysRevE.60.7186.
- [4] Provatas, N. and Elder, K. *Phase-Field Methods in Materials Science and Engineering*. Wiley-VCH: Weinheim, 2010. ISBN: 978-3-527-40747-7.
- [5] Xu, G. and Liu, Y. and Kang, Z. “Atomic Mobilities and Interdiffusivities for fcc Ni–Cr–Nb Alloys.” *Met. Trans. B* **47B** (2016) 3126–3131. DOI: 10.1007/s11663-016-0726-6.
- [6] Zhou, N.; Lv, D.; Zhang, H.; McAllister, D.; Zhang, F.; Mills, M. and Wang, Y. “Computer simulation of phase transformation and plastic deformation in IN718 superalloy: Microstructural evolution during precipitation.” *Acta Mater.* **65** (2014) 270–286. DOI: 10.1016/j.actamat.2013.10.069.